Cell-Specific Translational Profiling in Acute Kidney Injury

Jing Liu[1, 2, 4], A. Michaela Krautzberger[1, 2, 4], Shannan H. Sui[6], Oliver M. Hofmann[6], Ying Chen[1], Manfred Baetscher[1#], Ivica Grgic[7, 8], Sanjeev Kumar[1, 2, 4], Benjamin Humphreys[7], Winston A. Hide[6], Andrew P. McMahon[1, 2, 3, 4, 5*]

1. Dept. of Molecular and Cellular Biology, Harvard University, Cambridge, MA, USA
2. Dept. of Stem Cell and Regenerative Biology, Harvard University, Cambridge, MA, USA
3. Harvard Stem Cell Institute, Harvard University, Cambridge, MA, USA
4. Dept. of Stem Cell Biology and Regenerative Medicine, Keck School of Medicine of the University of Southern California, Los Angeles, CA, USA
5. USC Stem Cell, University of Southern California, Los Angeles, CA, USA
6. Dept. of Biostatistics, Harvard School of Public Health, Harvard University, Boston, MA, USA
7. Renal Division, Department of Medicine, Brigham and Women's Hospital, Harvard Medical School, Boston, MA, USA
8. Department of Internal Medicine and Nephrology, Philipps-University, Marburg, Germany

Present Address: Manfred Baetscher, 6900 SE 35th Ave, Portland, OR, USA

Authorship note: Jing Liu and A. Michaela Krautzberger contributed equally to this work.

Conflict of interest:

Research on kidney injury in the McMahon and Humphreys laboratories is supported by Evotec International, Germany.

*** Correspondence:**

Andrew P. McMahon, Ph.D.

Department of Stem Cell Biology and Regenerative Medicine,

Broad-CIRM Center,

Keck School of Medicine, University of Southern California

1425 San Pablo Street, Los Angeles, 90089.

Phone (323) 442-3056

Fax (323) 442-8024

E-mail: amcmahon@med.usc.edu

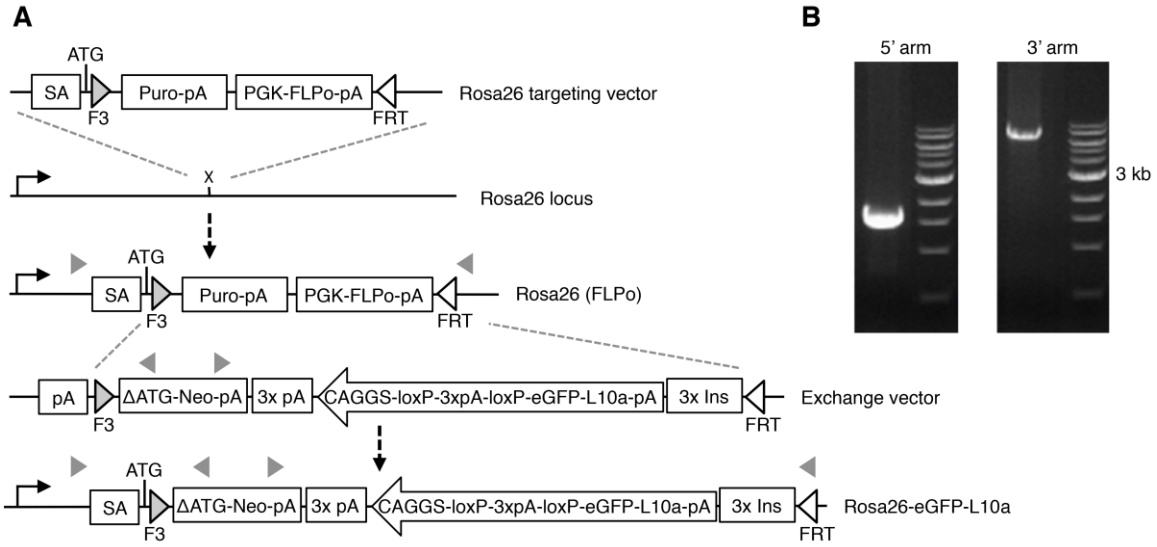

Supplemental Figure 1

Schematic of targeting strategy used for insertion of the eGFP-L10a expression cassette into the Rosa26 locus through RMCE (recombinase-mediated cassette exchange). (**A**) The CAGGS-loxP-3xpA-loxP-eGFP-L10a-pA transgene expression cassette was reversely integrated into the Rosa26 locus. SA, splice acceptor; ATG, translation initiation codon; F3/FRT, recombination sites; PGK, phosphoglycerokinase promoter; Puro, puromycin resistance gene; pA, SV40 polyadenylation/transcriptional stop signal; FLPo, codon-optimized FLP recombinase; Ins, 400 bp core region of chicken β-globin insulator; ΔATG-Neo, promoter/ATG-less neomycin resistance gene. (**B**) Correct targeting was confirmed by PCR. Gray arrowheads in (A) indicate primer binding sites used for PCR screening.

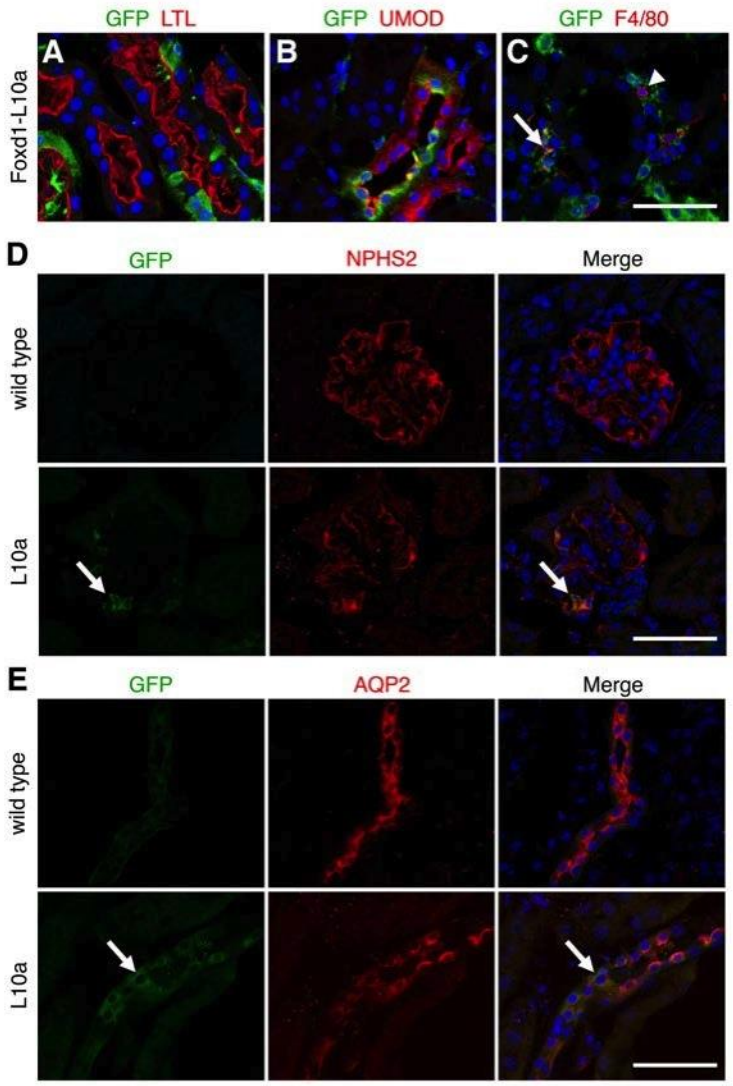

Supplemental Figure 2
GFP expression in Foxd1-L10a and L10a adult kidneys. (**A-C**) Immunofluorescence analysis of GFP expression in Foxd1-L10a kidneys shows sporadic induction in (**A**) LTL-positive proximal tubules, (**B**) uromodulin (UMOD)-positive thick ascending limbs of loop of Henle, and (**C**) in a subset of F4/80-positive macrophages (arrow). Arrowhead shows a GFP-negative, F4/80-positive macrophage. (**D-E**) Comparison of L10a kidneys to wild-type specimens reveals GFP expression in L10a kidneys in (**D**) Podocin (NPHS2)-positive podocytes (arrow) and (**E**) in a subset of aquaporin 2 (AQP2)-positive collecting duct cells (arrow). Nuclei are stained with Hoechst (blue) in all images. Scale bars: 50 µm.

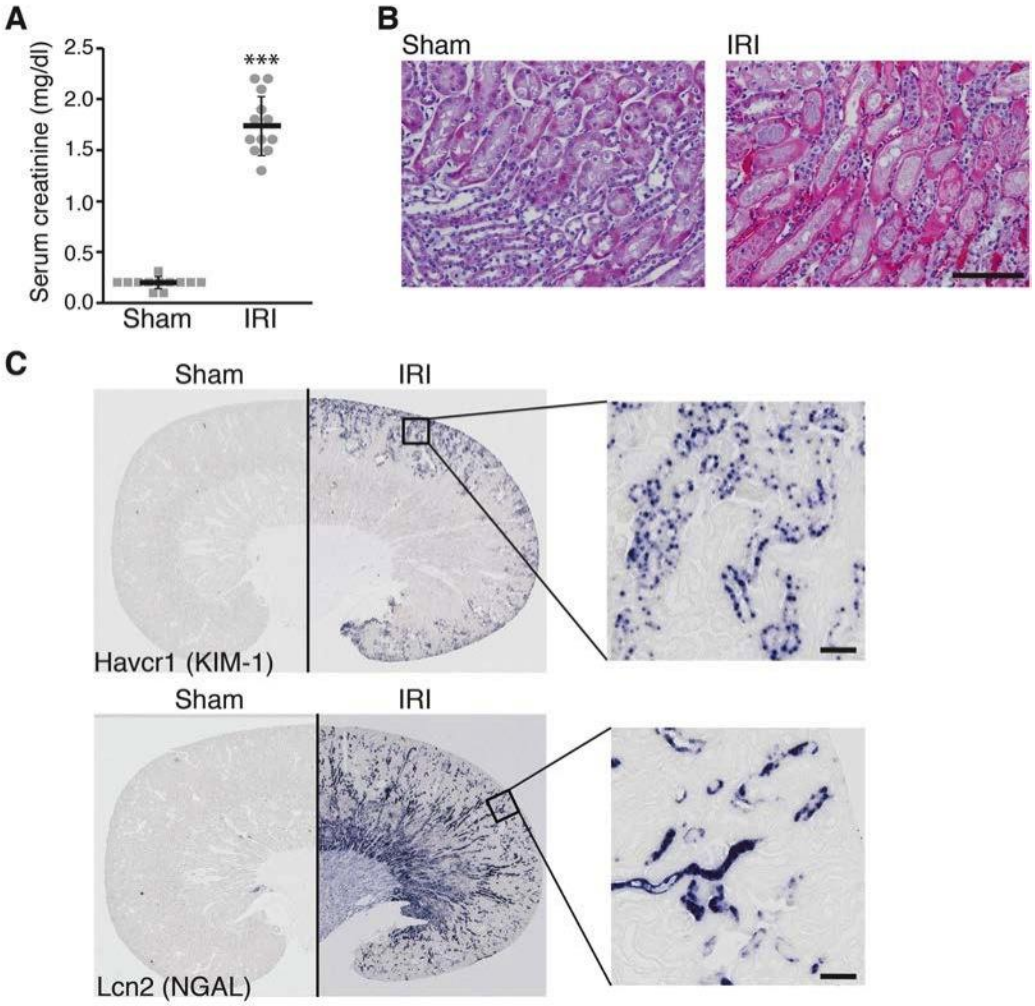

Supplemental Figure 3
Significant renal injury in 28-min IRI model**. (A**) Serum creatinine levels are significantly increased 24 hours post IRI. ****P* < 0.001 (n=12/group; mean ±SEM). (**B**) Representative hematoxylin and eosin–stained images from the outer medulla show severe damage of tubular cells in IRI kidneys. (**C**) RNA in situ hybridization confirmed induction and showed distinct expression patterns for two novel biomarkers, *Havcr1* (encoding KIM-1) and *Lcn2* (encoding NGAL) 24 hours after IRI treatment. Scale bars: 100 µm.

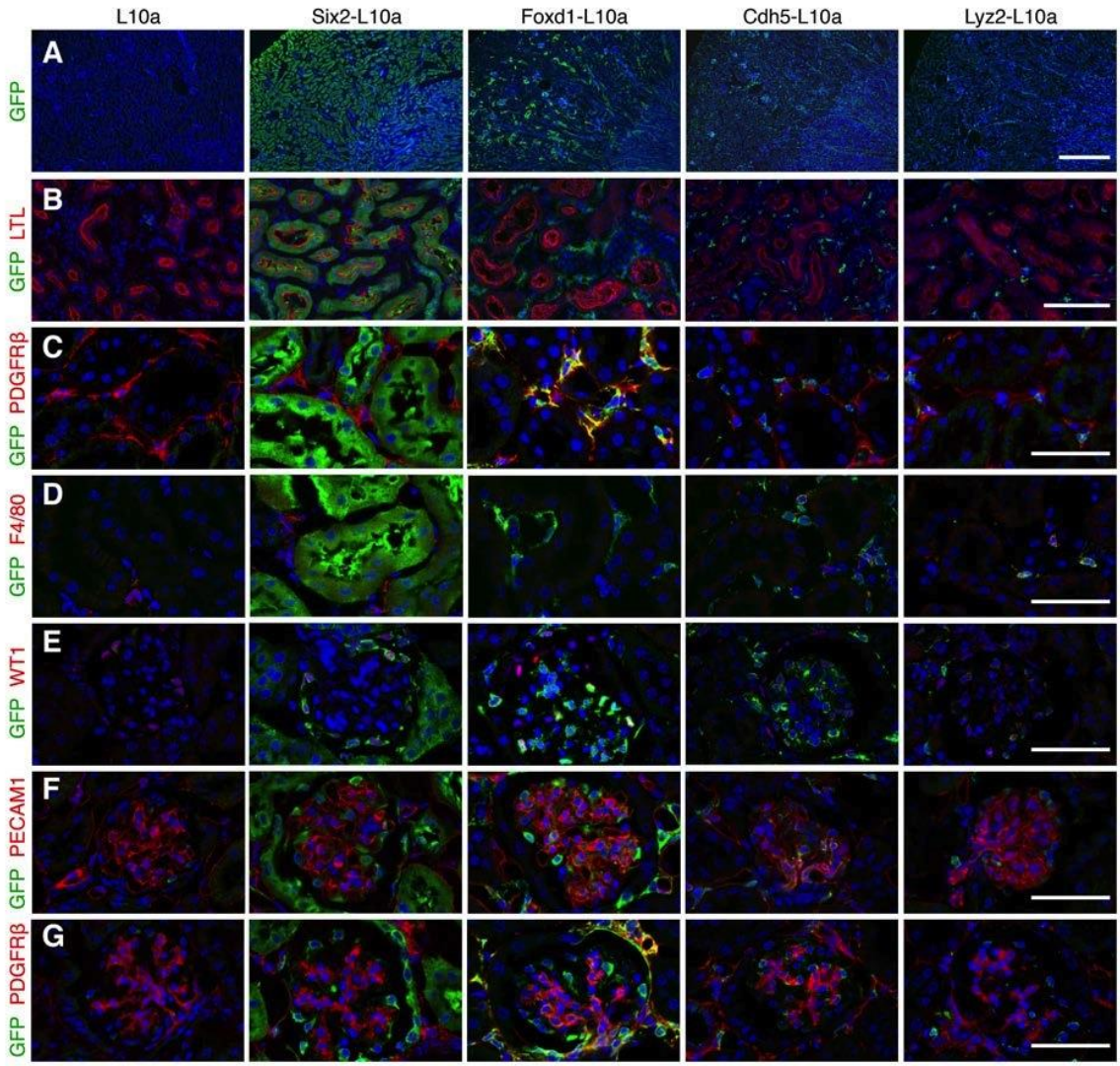

Supplemental Figure 4
Double immunofluorescence analysis with GFP and cell type-specific markers in sham-operated kidneys of four different CRE-L10a and L10a mice. (**A-G**) Representative images of GFP immunostaining (green) combined with cell type-specific antibodies (red): (**B**) LTL for proximal tubules, (**C** and **G**) PDGFRβ for interstitial cells (**C**) and mesangial cells (**G**), (**D**) F4/80 for macrophages, (**E**) WT1 for podocytes, and (**F**) PECAM1 for endothelial cells. Nuclei are stained with Hoechst (blue) in all images. Scale bars: 500 µm (**A**), 100 µm (**B**), 50 µm (**C**-**G**).

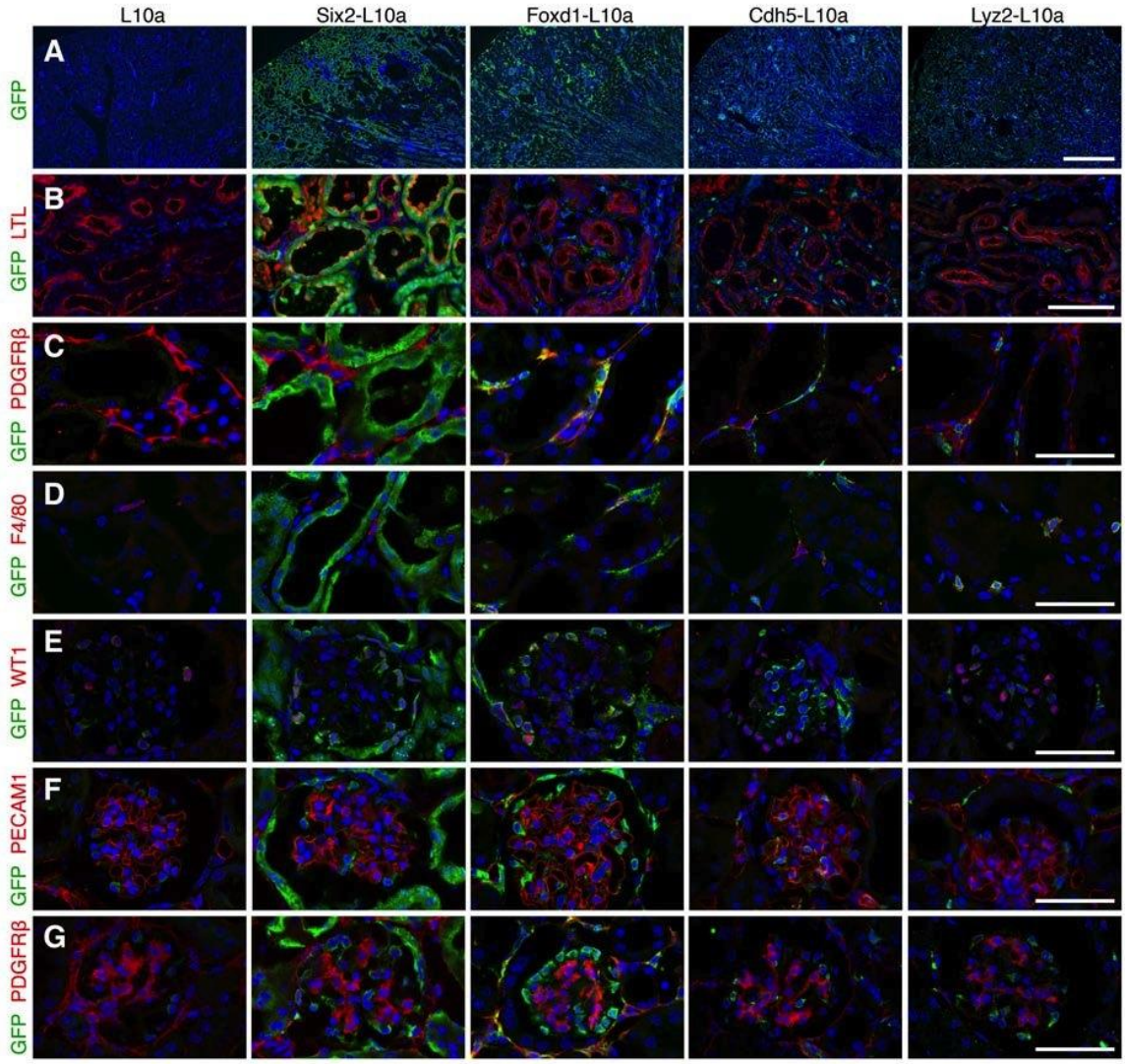

Supplemental Figure 5
Double immunofluorescence analysis with GFP and cell type-specific markers in IRI-treated kidneys of four different CRE-L10a and L10a mice. (**A-G**) Representative images of GFP immunostaining (green) combined with cell type-specific antibodies (red): (**B**) LTL for proximal tubules, (**C** and **G**) PDGFRβ for interstitial cells (**C**) and mesangial cells (**G**), (**D**) F4/80 for macrophages, (**E**) WT1 for podocytes, and (**F**) PECAM1 for endothelial cells. Nuclei are stained with Hoechst (blue) in all images. Scale bars: 500 µm (**A**), 100 µm (**B**), 50 µm (**C**-**G**).

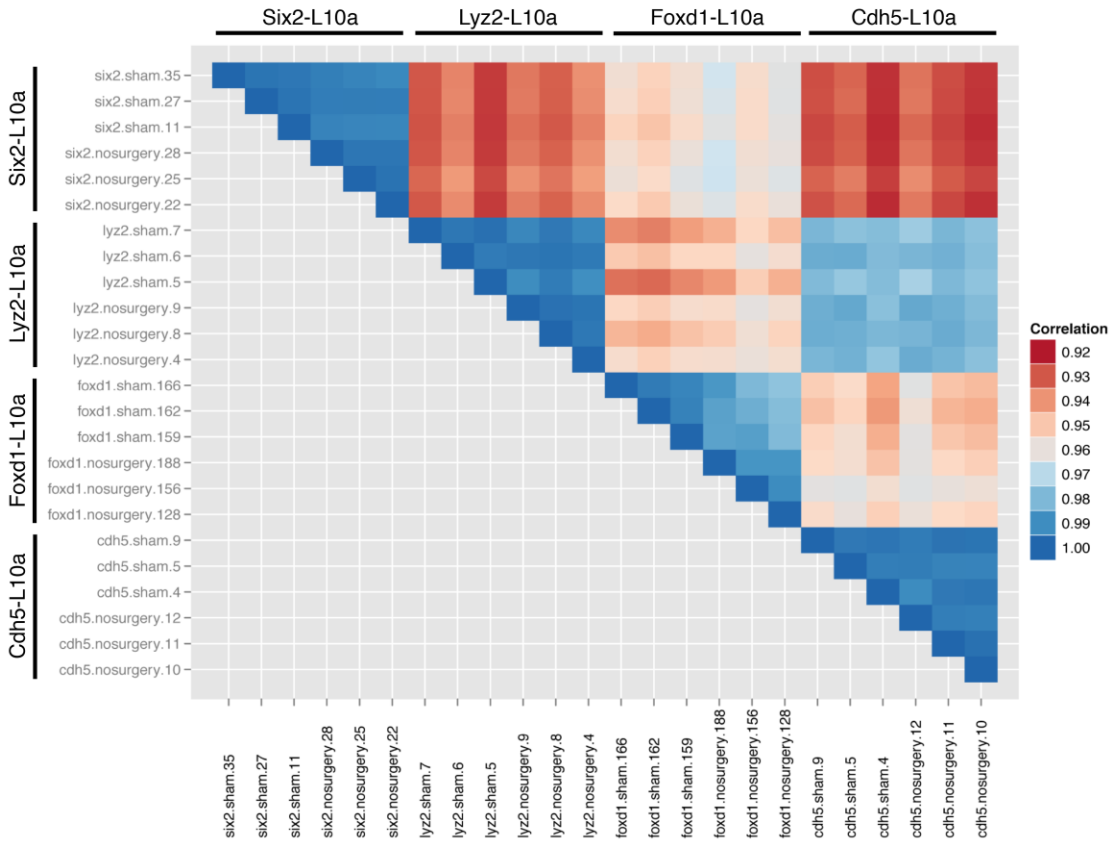

Supplemental Figure 6
Correlation matrix of TRAP no-surgery and sham-surgery samples. High correlation is observed amongst biological replicates for no-surgery and sham-surgery (mean correlation: 0.96). High correlation is also observed between Cdh5-L10a and Lyz2-L10a samples due to overlapping CRE activity in the myeloid cell lineage.

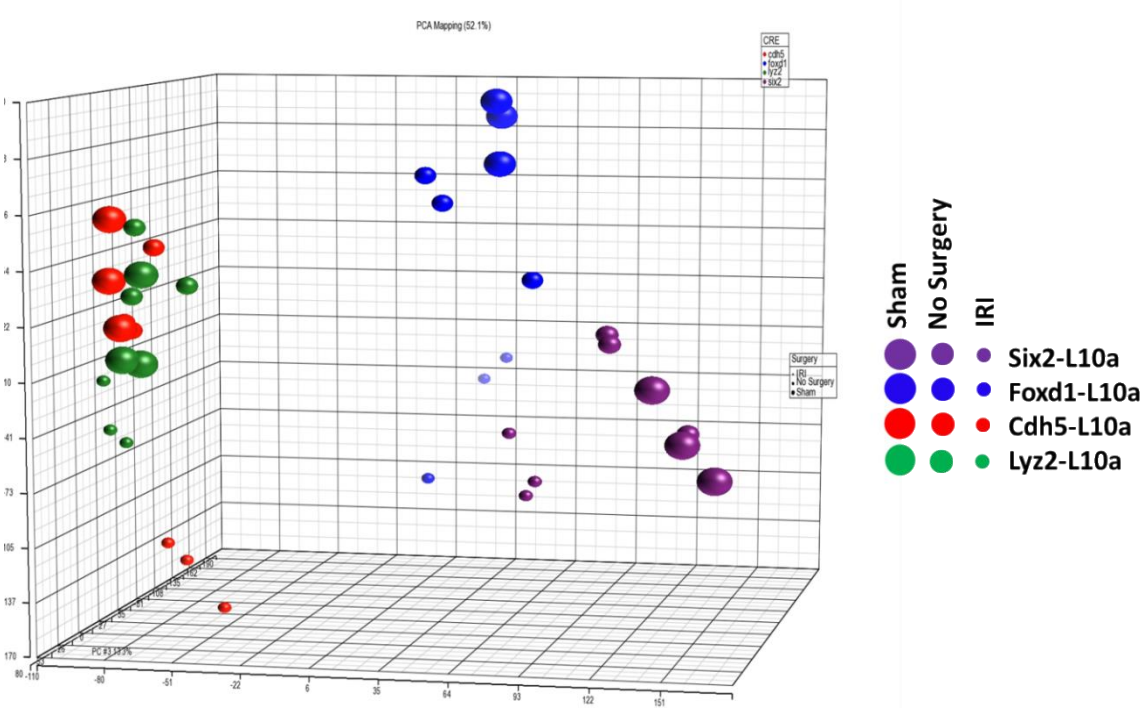

Supplemental Figure 7
Principle Component Analysis (PCA) plot shows tight clustering of biological replicates and distinct clustering between IRI and no-surgery/sham-surgery conditions.

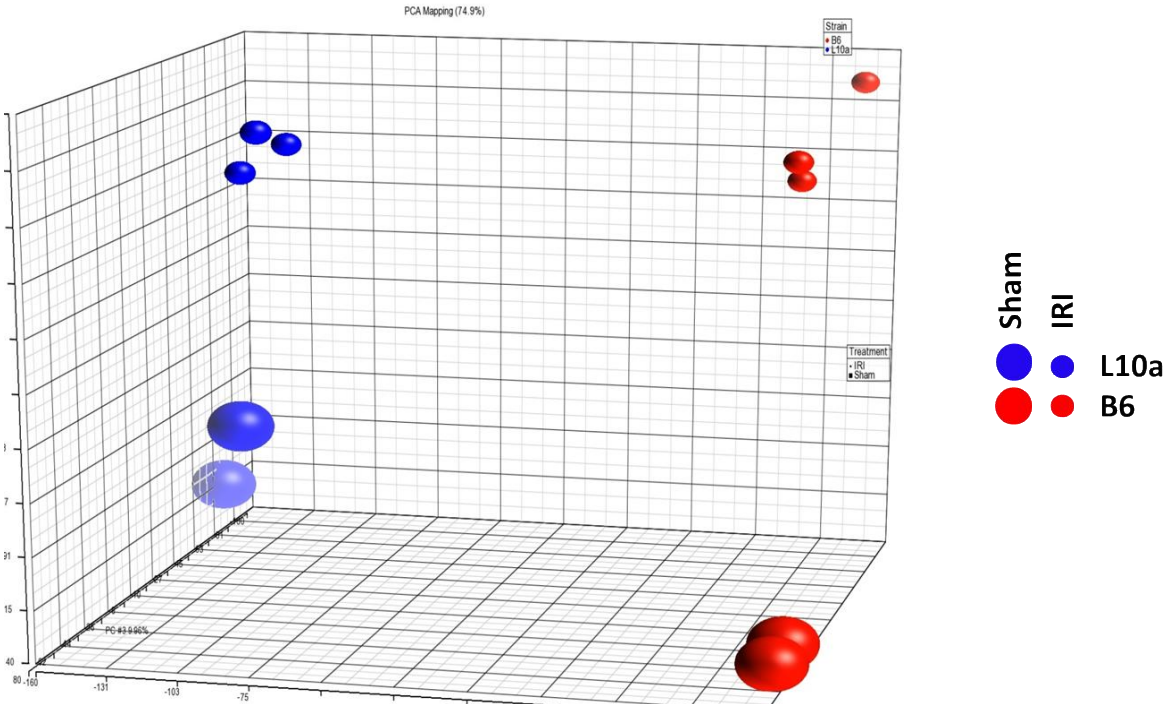

Supplemental Figure 8
Principle Components Analysis (PCA) plot for L10a vs. wild-type C57/BL6 TRAP microarray samples illustrates diversity between the two data sets. (Sham-surgery: two biological replicates; IRI treatment: three biological replicates).

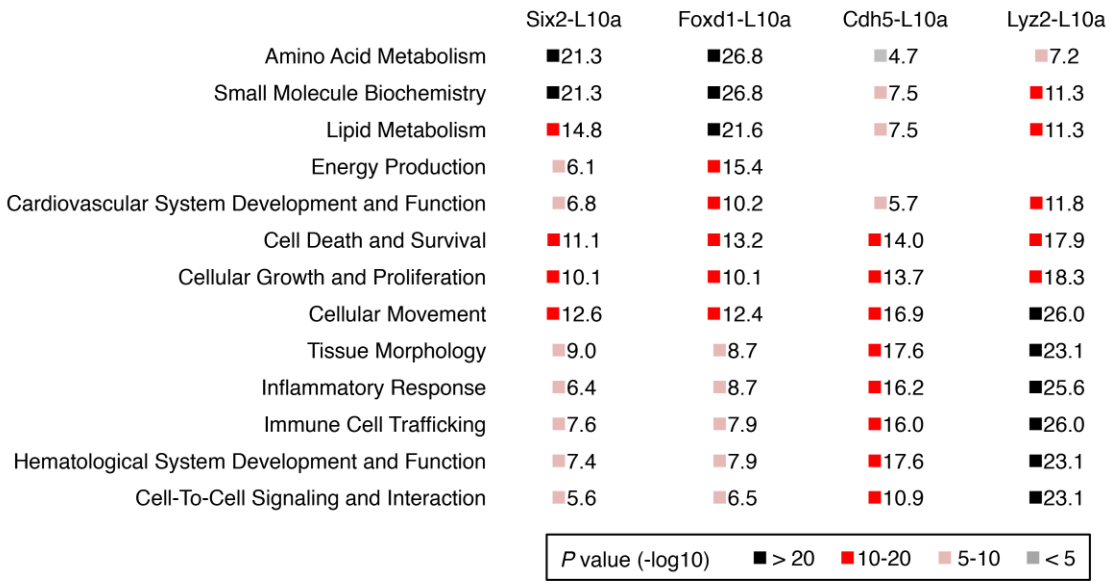

Supplemental Figure 9
Ingenuity Biological Function analysis of differentially expressed genes (IRI vs. Sham) within each of the four CRE-L10a populations.

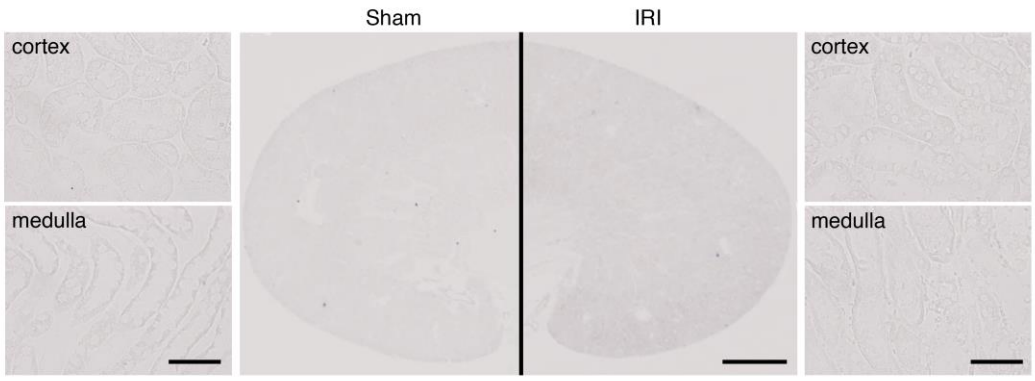

Supplemental Figure 10
Control experiments for RNA in situ hybridization. Sham-operated and IRI kidneys show no signal in a no-probe RNA in situ hybridization control experiment. Scale bars: 1 mm (overview), 50 µm (high-power views).

CRE	eGFP-L10a expression	TRAP yield (µg/kidney)
Six2	Tubular epithelial cells	4±0.7
	Podocytes	
Foxd1	Fibroblasts	1.5±0.3
	Pericytes	
	Vascular smooth muslce cells	
	Mesangial cells	
	Podocytes	
	Subset of tubular cells	
	Subset of macrophages	
Cdh5	Endothelial cells	0.25±0.04
	Macrophages	
Lyz2	Macrophages	0.13±0.02
	Monocytes	
	Granulocytes	
	Dendritic cells	
L10a	Podocytes	~0.03
	Subset of collecting duct cells	

Supplemental Table 1
eGFP-L10a expression in specific cellular compartments of the kidney in four CRE-activated and L10a lines and the corresponding TRAP RNA yields.

	Gene Number	**Six2**	**Foxd1**	**Cdh5**	**Lyz2**
	Up and Down	1032[a]	1614[a]	1615[a]	896[a]
Up	Six2	435[b]	197	131	110
	Foxd1		540[b]	208	145
	Cdh5			535[b]	197
	Lyz2				446[b]
Down	Six2	597[c]			
	Foxd1	409	1074[c]		
	Cdh5	137	299	1080[c]	
	Lyz2	142	234	209	450[c]

Supplemental Table 2
Comparison of numbers of differentially expressed genes (IRI vs. Sham) identified from TRAP among four CRE-L10a lines. [a]: Numbers of differentially expressed genes; [b]: upregulated; [c]: downregulated genes in each of the CRE-L10a lines and the numbers of shared genes between any two CRE-L10a lines were shown.